The influence of the entry speed to flow field above water surface on the water entry phenomenon

Takamasa Kikchi[1], KazuyoshiTakayama[2]
[1](College of Science and Technology, Nihon University, Japan)
[2](Engineering, Tohoku University, Japan)

ABSTRACT : *To evaluate the influence of the entry speed to flow field above the water surface on an object high-speed entering into water, the flow field was measured experimentally by using an optical visualization method. The entry speed was ranging from 0.2 to 1.5 km/s. In case that the entry speed was higher than the sound speed of gas above the water surface, the vertical velocity of the tip of a water splash was linear to the vertical location of the tip. The ratio between the initial vertical velocity of a water splash and the entry speed was independent from the entry speed and was constant.A shock wave was driven above the water surface by the entry even thoughthe entry speed was lower than the sound speed of gas above the water surface.A scaling law for the propagation of a shock wave driven by explosion of an explosive was applicable to the propagation of the shock wave driven by the water entry by using the kinetic energy of the entry object instead of the explosive energy.*

KEYWORDS –*water entry, shock wave, visualization, ballistic range*

I. INTRODUCTION

We are interested in phenomena generated by water entry of an object. The water entry phenomenon is a complex unsteady flow including multiphase and gas/liquid surface deformation. As studies of an underwater projectile and cavity phenomena at low entry speed, experimental studies of hydroballistics are known[1]. May discussed quantitatively the interrelationship of each phenomenon on the water entry at relatively low entry speed[2]. As studies of the water entry at high entry speed, McMillen discussed about the shape of an underwater shock wave visualized by using single micro-spark[3]. Shi et al. shot, by a rifle, a lead bullet into water at entry speed 340 m/s and observed the bullet motion by diffused light and measured the pressure at some depth[4]. At higher entry speed, only numerical simulation results are known[5]. Hence, to evaluate the influence of the entry speed on the high speed water entry phenomena experimentally is essential research issues. In case of impact to solid, fragment ejecta only spreads into radial direction[6]. In case of impact to liquid, splash spreads into radial direction and moves back to impact axis, then closes. This closure above the liquid surface, is called the surface closure, caused by differential pressure between inside and outside of the splash [7]. At entry speed higher than the sound speed of gas above the water surface, a shock wave exists around an entry object. So, to clarify the phenomena above the water surface, discussion from fluid dynamical and shock dynamical point of view is necessary. The optical visualization method is suitable to observe compressible flow accompanying a shock wave. We observed the flow field above the water surface by using the shadow graph method which was one of the optical visualization method. From images, the influences of the entry speed on water splash generation and the flow field above the water surface are discussed.

II. EXPERIMENT

2.1 Experimental facility and projectile

The experiments were performed in an oblique ballistic range (vertical entry mode) in the Institute of Fluids Science, Tohoku University. The ballistic range is illustrated in Fig. 1. This ballistic range is a small gas/powder gun. The mount in which a barrel, a free-flight section and a test section are fixed is able to be lifted by a screw jack. The projectile was a SUS304 sphere of 5.0 mm in diameter and 0.52 gram in mass. It was installed into a 4-parts type polycarbonate sabot of 10 mm in diameter and 12 mm in length. The projectile and the sabot are shown in Fig. 2.

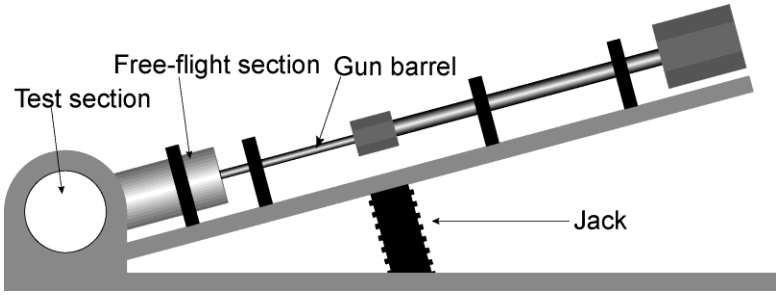

Fig. 1. Schematic diagram of the oblique ballistic range used in the experiments

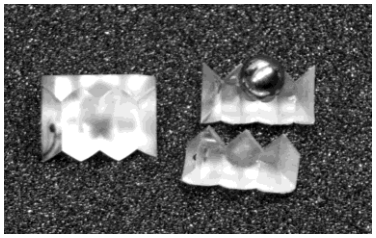

Fig. 2. A projectile and a 4-parts sabot

2.2Experimental description

The experimental description is illustrated in Fig. 3. The sabot including the projectile was accelerated by helium gas/powder combustion gas and was launched from the gun muzzle. The sabot and the projectile flied in the free-flight section. The sabot, whose front shape was inverse cone, suffered large drag force of air. The drag force pushed sabot parts out to the radial direction and the sabot parts separated from the projectile automatically. The separated parts were stopped by the collision to a sabot remover which was a thick steel plate with a hole at the center. Only the projectile passing through the hole went to the test section. Six baffle plates set in the free-flight section attenuated muzzle blast wave released from the gun muzzle. Since high-pressure driver gas which accelerated the projectile was vented into a dump tank from a hole at the side wall of the free-flight section, disturbance induced by driver gas pressure was negligible. The stainless water tank set in the test section was box shape of 320 mm in width, 100 mm in depth and 280 mm in height. The tank had acrylic windows for optical visualization at both sides. The water depth was fixed at 105 mm. The experimental conditions are shown in Table 1.

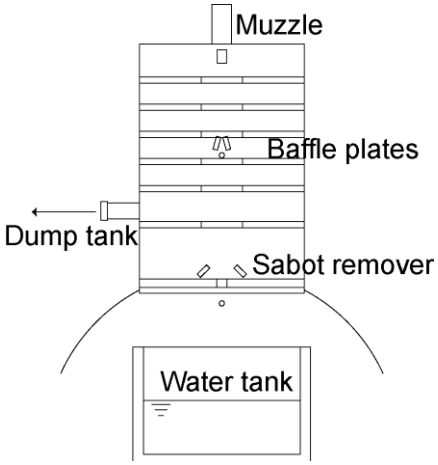

Fig. 3. Schematic diagram of the experimental description

Table 1 Experimental condition

Entry speed	0.2~0.5 km/s	0.5 ~ 1.5 km/s
Projectile	SUS304 sphere of 5.0 mm in diameter	
Acceleration source	Helium gas pressure	Smokeless powder
Light source	Metal halide lamp	
Camera	Phantom V7.3 (Vision Research Inc.)	HVP-1 (Shimadzu Co.)
Frame rate [fps]	21,052	250,000
Exposure time[μsec]	1.0	0.5

2.3 Visualization

The optical arrangement of shadow graph method is illustrated in Fig. 4. Light from a light source which was a metal halide lamp (PCS-UMX350, NIPPON.P.I.Co, Ltd) collimated by using a schlieren parabolic mirror of 300 mm in diameter. The parallel light passing through flow field converged by using a schlieren parabolic mirror. Then, visualization images were recorded by a high-speed video camera.

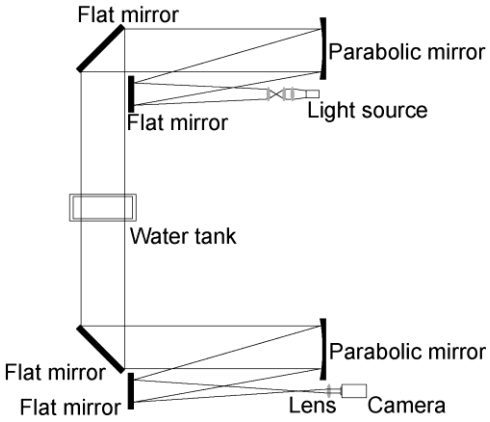

Fig. 4. Schematic diagram of the optical arrangement of shadow graph (plane view)

III. RESULTS AND DISCUSSION

3.1 Visualization image

The visualization images are shown in Fig. 5. The detail condition is shown in Table 1. The entry speed of the projectile was obtained from visualization images. In air above the water surface, a water splash was generated by the entry, a shock wave was driven around the water splash. This shock wave was observed even if the entry speed was lower than the sound speed of air.

3.2 The motion of the water splash

The motions of the water splash are illustrated in Fig. 6. The splash spread with time. The tip of the splash rolled downward (a). A water column formed beneath the splash (b). By rising of the water column, the rolling splash divided into two parts which were an upper part and a lower part. The upper splash was connected with the water column (c). A vortex ring was induced between the two parts of the splash. The upper splash started closing toward the entry trajectory (d). The spread upper splash closed completely at the entry trajectory. Finally, one water column formed (e). The time evolution of the vertical velocity of the tip of the upper splash against the vertical location is shown in Fig. 7. The ordinate designates the vertical velocity, the abscissa designates the vertical location from the water surface. The vertical velocity $v$was linear to the vertical location $x$as follows:

$$v = \alpha x + \beta \quad (1)$$

The coefficient α and β were obtained by the least square method. The value of β means the initial vertical velocity of the upper splash. The value of α and β against the entry speed are shown in Fig. 8. The ordinate designates the value of α and β, the abscissa designates the entry speed. Both α and β were linear to the entry

speed and the initial vertical velocity of the upper splash was lower than the entry speed. Hence, the ratio of velocities which are the initial vertical velocity of the upper splash and the entry speed is independent from the entry speed and is constant. The motion of the upper splash at all entry speed was able to be approximated by the equation (2) which was primitive function about time after the entry *t*of the equation (1).

$$x = \frac{\beta}{\alpha}(e^{\alpha t} - 1) \qquad (2)$$

The comparison of the approximation and the experiment is shown in Fig. 9. The ordinate designates the vertical location from the water surface, the abscissa designates time after the entry. Two values agreed well except for entry speed lower than the sound speed of air. Hence, the tendency of the water splash motion changes when the entry speed exceeds the sound speed of gas over the water surface.

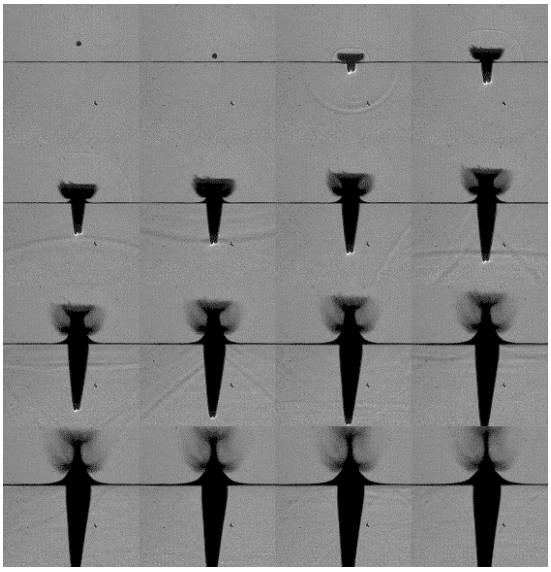

The entry speed; 256.05 m/s
The frame interval; 47.5 μsec

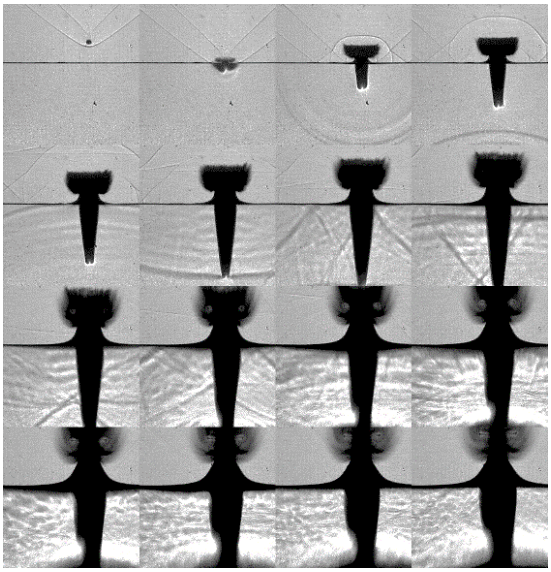

The entry speed; 463.93 m/s
The frame interval; 47.5 μsec

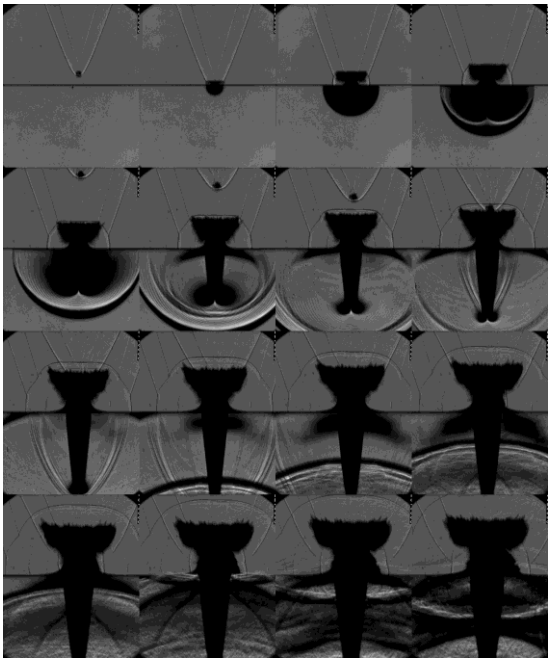

The entry speed; 1141.7 m/s
The frame interval; 12.0 μsec

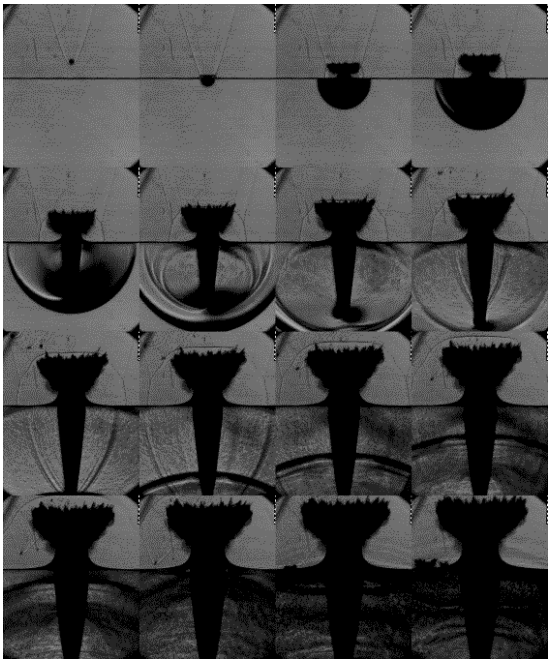

The entry speed; 1514.8 m/s
The frame interval; 12.0 μsec

Fig. 5. Sequential photographs in shadow graph method

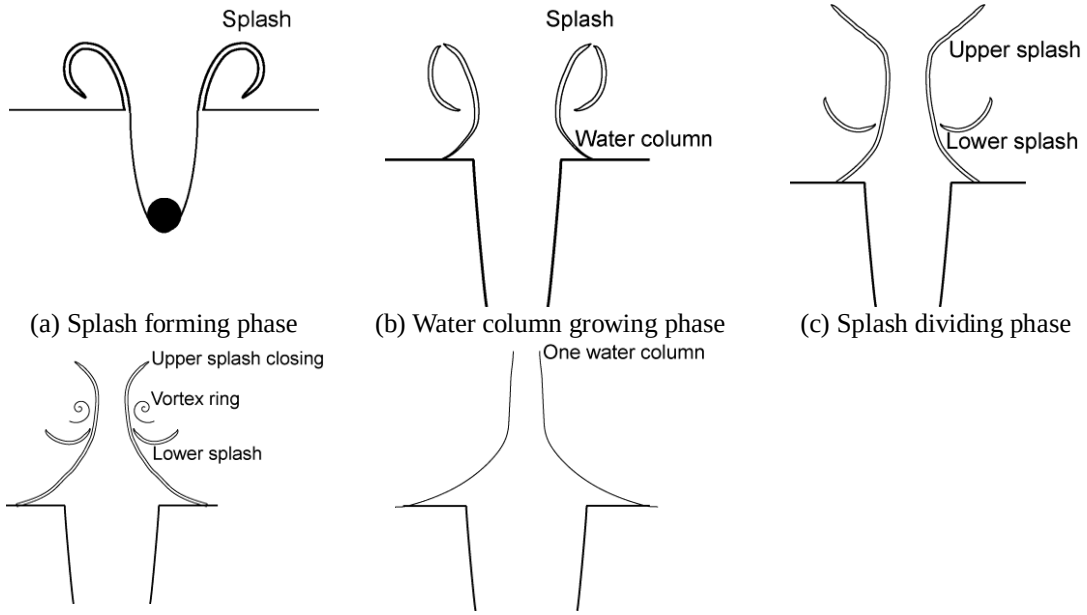

(a) Splash forming phase (b) Water column growing phase (c) Splash dividing phase

(d) Splash closing phase (e) Splash closed phase

Fig. 6. Detail of the splash motion

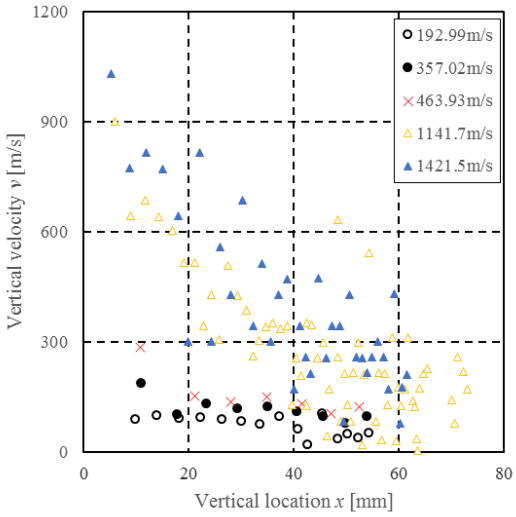

Fig. 7. Vertical velocity vs vertical location of tip of the upper splash

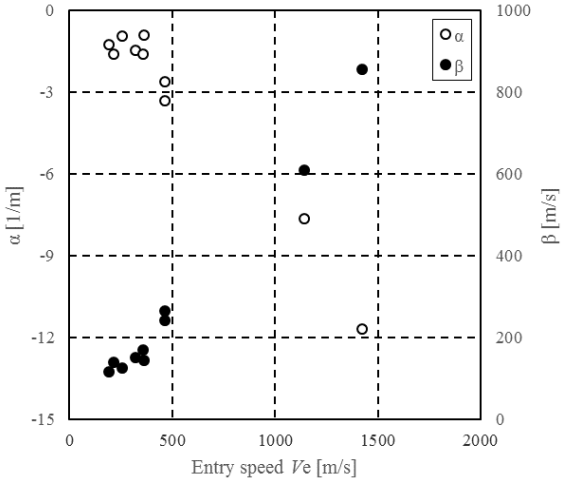

Fig. 8. α, β vs the entry speed

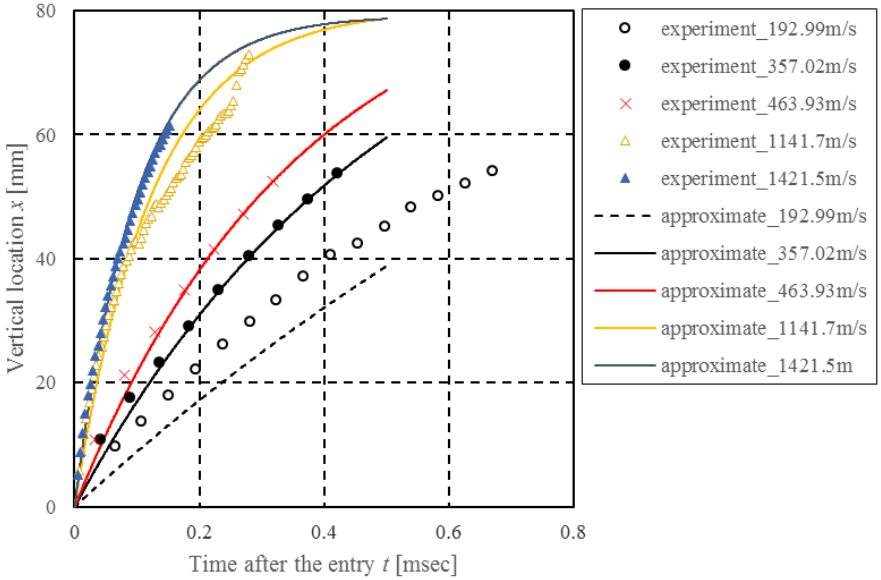

Fig. 9. Comparison of the approximation and the experiment

3.3The shock wave in air above the water surface

Since a shock wave after the entry was observed above the water surface even though the entry speed was lower than the sound speed of air, this shock wave is not a shock wave around the projectile but a shock wave caused by the entry. On an explosion of an explosive, instantaneous vaporized and expanded combustion gas compresses air as a piston and drives a shock wave. The splash expressed the same shock wave drive effect as the explosion. A scaling law that the distance is divided by the cube root of explosive mass is used to the propagation of a spherical shock wave driven by explosion:

$$R_S = \frac{R}{S}$$
$$t_S = \frac{ct}{S} \tag{3}$$

where, R and R_S is the actual and the normalized radius of a spherical shock wave respectively and t_S is the actual and the normalized time after explosion. The coefficient S and c are given as follows:

$$S = \left(\frac{W}{1}\right)^{1/3}\left(\frac{101.325}{P}\right)^{1/3}$$
$$c = \frac{a}{a_0} = \left(\frac{T}{288.16}\right)^{1/2} \tag{4}$$

where, W is the mass of an explosive, P is the ambient pressure, a is the ambient speed of sound, a_0 is the speed of sound at the normal state and T is the ambient absolute temperature. On TNT explosion, this law agrees well

at wide range of both the mass of an explosive and environmental conditions [8]. Since the energy of an explosive is proportional to the molar number of the explosive, the ratio of masses is same as the ratio of the energies and W in equation (4) is the energy contributed to explosion. The kinetic energy of an entry projectile is considered as this energy, then S in equation (4) can be rewritten as follows:

$$S = \left(\frac{\frac{1}{2}mV_e{}^2}{1}\right)^{1/3} \left(\frac{101.325}{P}\right)^{1/3} \quad (5)$$

where, V_e is the entry speed and m is the mass of the projectile.A shock wave at the entry trajectory was influenced from wake flow of the projectile, while a shock wave at the water surface left from the splash immediately after the entry. The time evolution of the horizontal location of the shock wave front at the water surface, which is shown in Fig. 10, before and after normalization are shown in Fig. 11. The horizontal location of the shock wave front was able to agree with thisscaling law. The normalized horizontal data were corresponding to the approximation curve of a spherical shock wave propagation presented by Dewey[9]:

$$R_S = A + Ba_0t_S + C\ln(1 + a_0t_S) + D\sqrt{\ln(1 + a_0t_S)} \quad (6)$$

where, A, B, C, D are coefficient. By multiple regression analysis, the value of coefficients was A = 4.970437, B = 0.972195, C = 6.069949, D = -3.71615. Hence, the flow field induced on high-speed water entry is similar to the explosion of an explosive and the scaling law for explosion is able to apply to the driven shock wave propagation by using the kinetic energy of the projectile instead of the energy of an explosive.

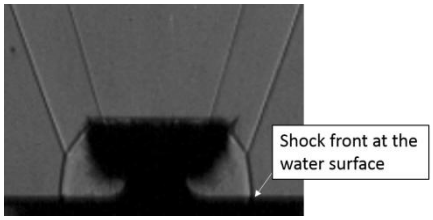

Fig. 10. Shock wave front at the water surface

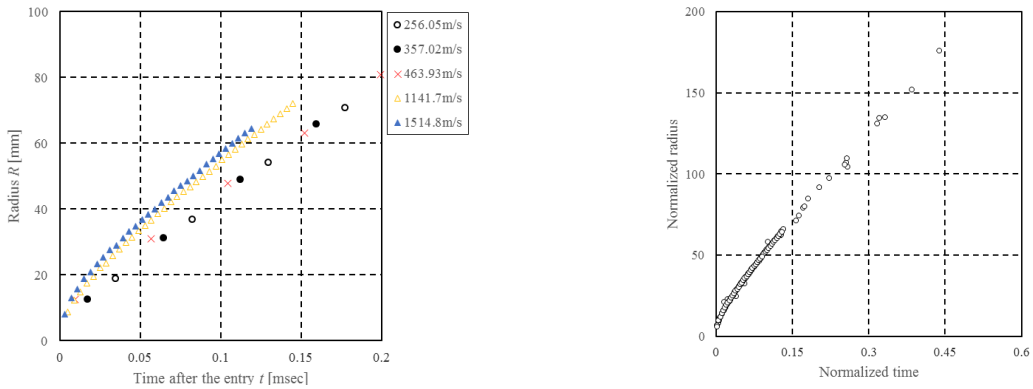

(a) Before normalization (b) After normalization

Fig. 11 Horizontal location of the shock wave front in air vs time after the entry

IV. CONCLUSION

The flow field above the water surface on high-speed water entry was visualized by using the shadow graph method and a high-speed video camera. Then, the influence of the entry speed to phenomena was discussed quantitatively. The obtained results are summarized as follows:

- The tendency of the water splash motion changes when the entry speed exceeds the sound speed of gas over the water surface. In case of the entry speed exceeding the sound speed of the gas, the splash vertical velocity is linear to the splash vertical location, and the ratio between the splash initial velocity and the entry speed is independent from the entry speed and is constant.
- A shock wave is driven by the splash like the explosion of an explosive even thoughthe entry speed is lower than the sound speed of gas above the water surface. The propagation of this shock wave agrees with a scaling law of the propagation of a spherical shock wave driven by the explosion of an explosive. In this

scaling, the kinetic energy of the projectile is used in place of the energy of the explosive.

V. Acknowledgements

I would like to express my sincere appreciation to Professor Shigeru Obayashi, Professor. KiyonobuOhtani, Professor Mingyu Sun of the Institute of Fluids Science, Tohoku University and Professor DaijuNumata of Tokai University for their valuable suggestion and comments. I would like to thank Mr. Toshihiro Ogawa, Mr. Kazuo Akama, Mr. ShokichiHayasaka, Mr. Kiyoshi Kikuta and Mr. MasatakaHonna of staffs in Tohoku University for their helps and technical advises.

REFERENCES

[1] John G. Waugh and G. W. Stubstad, *Hydroballisticsmodeling*(Naval Undersea Center, 1972).

[2] Albert May, Vertical Entry of Missiles into Water, *Journal of Applied Physics, 23(12),* 1952, 1362-1372.

[3] J. Haward McMillen, Shock Wave Pressures in Water Produced by Impact of Small Spheres, *Physical Review, 68(9),* 1945,198-209.

[4] Hong-Hui Shi and Makoto Kume, An experimental research on the flow field of water entry by pressure measurements, *Physics of Fluid, 13(1),* 2001, 347-349.

[5] M.D.Neaves and J.R.Edwards, All-Speed Time-Accurate Underwater Projectile Calculations Using a Preconditioning Algotithm, *Journal of Fluid Engineering, 128,* 2006, 284-296.

[6] R. Greeley, J. Fink, D. E. Gault, D. B. Snyder, J. E. Guest and P. H. Schultz, Impact cratering in viscous targets - Laboratory experiments, *Pro. 11th Lunar Planetary Science Conference*, USA, 1980, 2075-2097.

[7] David Gilbarg and Robert A. Anderson, Influence of Atmospheric Pressure on the Phenomena Accompanying the Entry of Spheres into Water, *Journal of Applied Physics, 19(2),* 1948, 127-139.

[8] Dewey JM, The air velocity in blast waves from t.n.t.explosions, *Proc Roy Soc A, 279,* 1964, 366-385.

[9] Dewey JM, The properties of a blast wave obtained from an analysis of the particle trajectories, *Proc Roy Soc A, 324,* 1971, 275-299